UDC 551.509.313

HEIGHT AND KINETIC ENERGY OSCILLATIONS IN A LIMITED-REGION PREDICTION MODEL

RUSSELL L. ELSBERRY and E. J. HARRISON, JR.
Naval Postgraduate School, Monterey, Calif.

ABSTRACT

A 10-level primitive-equation model designed for prediction of circulations within a limited region of the Tropics is described. The model is initialized from wind and temperature information. During the course of the integration two types of oscillations arose from the imposed horizontal boundary conditions—a short-period height oscillation and a longer period kinetic energy oscillation. The character of the two oscillations and the boundary conditions needed to remove the oscillations are described.

1. INTRODUCTION

Benwell and Bretherton (1968) have recently described an oscillation in the pressure field of a 10-level numerical prediction model. Diagnosis of the oscillation showed characteristics of a standing inertial-gravitational wave in the external mode. Inclusion of the linear terms in the balance equation solution for the initial winds almost completely eliminated the pressure oscillations. Murakami (1969) has examined the problem of determining the geopotential from the initial values of the stream function. For certain wavelengths, a solution to the linear equations that retains the Rossby waves but supresses the gravity waves is possible. Krishnamurti (1969) noted inertial-gravitation oscillations in a primitive equation model especially applied to tropical circulations with initialization from winds rather than height fields. These oscillations developed even though a rather detailed diagnostic balance model was used to define a consistent initial state. Krishnamurti notes that an adjustment of the wind and pressure occurs, with diffusion of momentum and potential temperature damping the smaller scale oscillations.

Some similar numerical experiments by the authors resulted in distortions in the predicted wind and pressure fields that had amplitudes comparable to those of the synoptic features. Initialization using wind fields for these experiments included the terms which eliminated the oscillations considered by Benwell and Bretherton (1968). The vertical motion is initially zero. In our experiments, the synoptic scale oscillations did not significantly damp with time because diffusion terms are not included. As the prognostic model was developed to test the effect of different latent heating parameterization schemes on the simulation of tropical disturbances, oscillations of the type described are very important. In general, the various parameterization schemes (e.g., Kuo 1965, Charney and Eliassen 1964, Rosenthal 1969, Pearce and Riehl 1968) depend on low-level convergence. The vertical motion induced by the rapidly moving gravity waves can mask that due to meteorological developments. In addition, the 24-hr surface pressure changes in the Tropics are generally small; consequently, a forecast based on a prognosis including these oscillations would fail unless the mode and phase of the waves were known.

A 19-hr oscillation in the total kinetic energy of the system was also a distinct and persistent feature of the experiments. Brown (1970) has detected a 10-hr period kinetic energy oscillation in the National Meteorological Center model. Brown found the initialization scheme to be the generating mechanism.

The objective of the present study is to describe the short-period height oscillation and the longer period kinetic energy oscillation produced in the primitive-equation model. Experiments with actual data and idealized flow patterns were performed to determine the origin of these oscillations and to suggest methods of elimination. As in the above references, the causes of the oscillations were related to data initialization.

2. DIAGNOSTIC-PROGNOSTIC MODEL

The prognostic model is kept as simple as possible to isolate the effects of various types of latent heating parameterization. The model equations are

$$\frac{\partial u}{\partial t}=-L_{(u)}+fv-m\frac{\partial \phi}{\partial x}-F_x, \tag{1}$$

$$\frac{\partial v}{\partial t}=-L_{(v)}-fu-m\frac{\partial \phi}{\partial y}-F_y, \tag{2}$$

$$\frac{\partial \theta}{\partial t}=-L_{(\theta)}+Q_L+Q_S-Q_R, \tag{3}$$

$$\frac{\partial q}{\partial t}=-L_{(q)}+M_E-M_P, \tag{4}$$

$$\frac{\partial \omega}{\partial p}=-m^2\left[\frac{\partial}{\partial x}\left(\frac{u}{m}\right)+\frac{\partial}{\partial y}\left(\frac{v}{m}\right)\right], \tag{5}$$

and $$\Delta\phi=\hat{\theta}c_p\Delta\left(\frac{p}{1000}\right)^{R/c_p} \tag{6}$$

where the flux differencing after Arakawa (1966) is used, that is,

$$L_{(s)}=m^2\left[\frac{\partial}{\partial x}\left(\frac{us}{m}\right)+\frac{\partial}{\partial y}\left(\frac{vs}{m}\right)\right]+\frac{\partial}{\partial p}(\omega s)$$

for a general variable s. The other variables have their usual meteorological significance. The frictional terms F_x and F_y in eq (1) and (2) are only applied at the 950-mb level and represent surface dissipative effects.

For these experiments, the drag coefficient was assumed to be a constant of 1.5×10^{-3}. In eq (3), Q_L, Q_S, and Q_R represent latent, sensible, and radiative heating, respectively. Although the results shown in the remainder of this paper are for an adiabatic version, the general model includes latent heat release as formulated by Kuo (1965). Sensible heating is calculated from the usual bulk transport expression and applied in the boundary layer (1000–900 mb). A simple radiation scheme in which average radiative values vary only with height is used to offset the other forms of heating. The profile generally approximates that found by Riehl (1962) for this region. Equation (4) is the moisture balance equation where M_E and M_P represent changes in specific humidity due to evaporation and precipitation, respectively. The evaporation is computed with the bulk transport expression using a sea-surface temperature analysis by Landis and Leipper (1968). All condensed moisture is assumed to be precipitated with the latent heat added in eq (3). The remaining equations are the continuity equation (5) and the finite-difference form of the hydrostatic equation (6) where Δ represents a vertical finite difference and $\hat{\theta}$ is the pressure average of potential temperature for each layer.

The grid, on a mercator projection true at 22.5°N with 32 points east-west and 15 north-south spaced at 154 km, is centered near 20°N, 68°W. There are 10 equally spaced pressure levels in the vertical with the upper level at 100 mb and the lower at 1000 mb. The time step for the model is 6 min with centered time steps after an initial forward time step.

The east-west boundary conditions are forced cyclic continuity after the manner of Krishnamurti (1969). The north-south boundaries are insulated free-slip walls. The lower boundary condition is given by

$$\frac{d\phi_{1000}}{dt}=0 \tag{7}$$

where ϕ_{1000} is the 1000-mb geopotential and the vertical pressure velocity, ω, is obtained at the appropriate levels by integrating eq (5) downward from 100 mb where $\omega=0$.

In the diagnostic phase, the stream function (ψ) is derived from

$$\nabla^2\psi=\zeta \tag{8}$$

where the right-hand side is a weighted average of relative vorticity computed from the analyzed wind field and from the thermal vorticity in the layer below. The nondivergent portion of the wind is then

$$\mathbf{V}_\psi=\mathbf{k}\times\nabla\psi. \tag{9}$$

The geopotential is obtained from the nonlinear balance equation

$$\nabla^2\phi=\nabla\cdot f\nabla\psi+2J\left(\frac{\partial\psi}{\partial x},\frac{\partial\psi}{\partial y}\right). \tag{10}$$

With the hydrostatic equation in the form of eq (6), the mean potential temperature $\hat{\theta}$ is calculated for the layer between two levels of independently determined geopotential values. Including the thermal vorticity as a forcing function on the right-hand side of eq (8) improved the vertical consistency of the potential temperature fields.

Two important features of the prognostic model are matched by the diagnostic model. The flow in the zonal direction is made cyclic, and, along the northern and southern boundaries of the channel, insulated free-slip walls are assumed. For example, at the wall placed midway between the northernmost gridpoints, with the index j increasing northward,

$$v_{j+1}=-\frac{m_{j+1}}{m_j}v_j \text{ and } u_{j+1}=u_j. \tag{11}$$

Thus, in the diagnostic model, the wall is a streamline, requiring that ψ is constant. Conservation of kinetic energy in the finite difference formulation requires

$$\phi_{j+1}=\phi_j \text{ at the northern wall}$$

and this condition was imposed in solving for the geopotential in eq (10). This condition implies that the potential temperature is also constant across the walls. Note that the conditions chosen here are those required to match the prognostic equations, and differ from those of Hawkins and Rosenthal (1965), which are designed to produce an accurate representation of the original winds. Hawkins and Rosenthal (1965) show that inclusion of the divergent portion of the wind improves the representation of the actual wind field, but experiments in which the initialization included divergent components are not discussed here.

3. SHORT-PERIOD HEIGHT OSCILLATIONS

Examination of the total kinetic energy led to discovery of the kinetic energy oscillation and prompted a detailed analysis of the height fields at various subintervals of the period. The geopotential averaged over the pressure surface varied less than 10 $m^2\cdot s^{-2}$ as might be expected from eq (7). Calculation of the root-mean-square deviation (RMSD) of the geopotential from the area-averaged mean did illustrate a short-period oscillation. Some indication

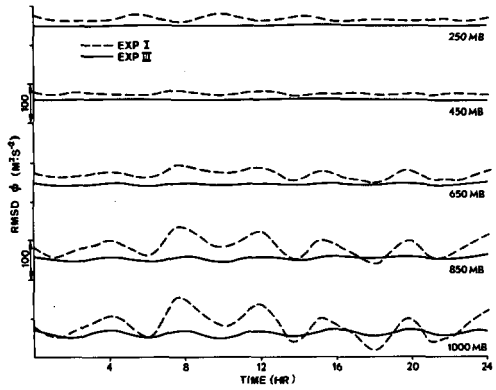

FIGURE 1.—Time variation of the root-mean-square deviations (RMSD) of the geopotential, ϕ, for selected pressure levels. Each of the curves is to the same scale with the ordinates displaced. See the text for differences between experiments I (dashed line) and III (solid line).

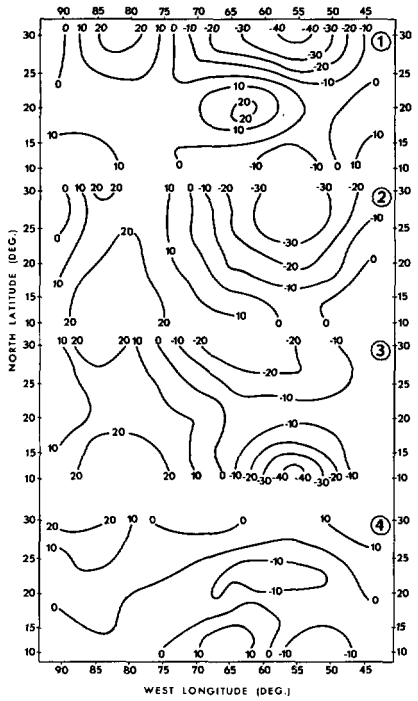

FIGURE 2.—Deviations from the initial 1000-mb height field (m) at: 1 hr (panel 1), 2 hr (panel 2), 3 hr (panel 3), and 4 hr (panel 4) from initial time of 1200 GMT on Aug. 29, 1965.

of a longer period variation in the RMSD of geopotential appears in figure 1, but the dominant period for experiment I is about 4 hr. The amplitude of the oscillation decreases from the 1000-mb level to 650 mb, then increases again at 250 mb, although the phase appears to be different at upper levels. An oscillation of 100 $m^2 \cdot s^{-2}$ represents a significant distortion of the geopotential on the pressure surface, especially at 1000 mb.

The evolution of deviations from the initial 1000-mb height field during the first cycle of the oscillation is shown in figure 2. The positive center to the right of the middle of

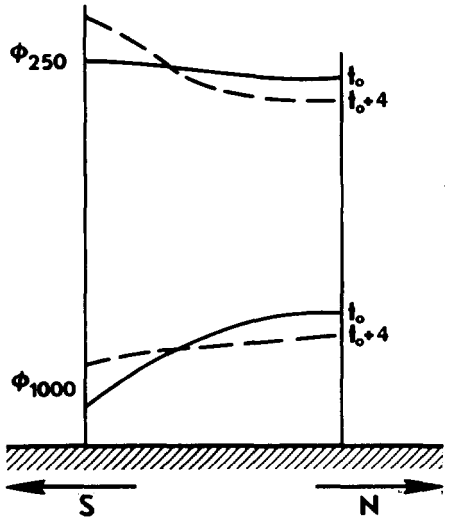

FIGURE 3.—Schematic of the variation in meridional height gradient at 1000 and 250 mb as a result of the short-period height oscillation. Variations in the zonal height gradient counterbalance the meridional gradient to restrict the area-averaged height to only small changes.

the grid corresponds to the position of tropical storm Betsy, the main synoptic feature of interest. By the end of the first hour (upper diagram in fig. 2), the storm has been predicted to fill nearly 25 m from an initial 1000-mb height value of 98 m. To the northeast, the extension of the Bermuda high has deepened more than 25 m from a value of 175 m. Compensation occurs farther to the west where the pressures are predicted to rise 25 m in 1 hr, so the area-averaged height changes by only 0.1 m. The rapid evolution of the rise and fall centers during the subsequent 3 hr is evident in the other sections of figure 2. At various times in the cycle, the centers near the northern and the southern boundaries dominate, but near the end of the cycle (hour 4 in fig. 2) the magnitude of the deviations is diminishing. It is then easy to see why 12-hr and 24-hr predicted height fields appeared quite reasonable and masked the existence of the oscillation.

Deviations from the initial height fields at other levels (not shown) closely reflect those in figure 2, but with larger amplitudes as suggested by the theory of Benwell and Bretherton (1968).

For the case shown in figure 2, the trade easterlies are replaced by westerlies aloft. The gravity wave oscillation produces a zonal height gradient which alternately diminishes and reinforces the normal synoptic pressure gradient. As the thickness (temperature) between the two levels is not substantially affected by the waves, the upper-level height gradient is increased when the low-level height gradient is diminished. Figure 3 is a schematic representation of the variations in height gradients. Since the meridional gradients (not shown) are also experiencing compensating changes, we find only a small kinetic energy oscillation with a 4-hr period.

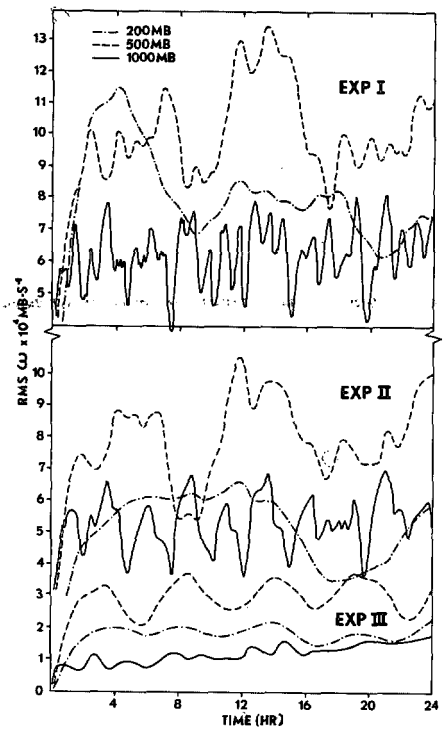

FIGURE 4.—Root-mean-square ω (10^{-4} mb·s^{-1}) as a function of time at: 1000 mb (solid line), 500 mb (dashed line), and 200 mb (dot-dash line) for each of the three experiments described in the text.

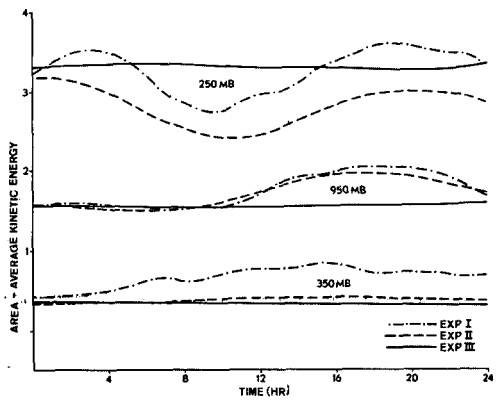

FIGURE 5.—Kinetic energy (J· cm^{-2}) at selected levels for experiment I (dash-dot line), experiment II (dashed line), and experiment III (solid line).

It should be noted that the character of the oscillation is quite distinct from that shown in figure 3 of Benwell and Bretherton (1968). In their model, the heights are fixed on the boundary and the maximum amplitude is in the center of the region. With no compensation between pressure rises and falls, large height variations occur even when averaged over the entire region. As Benwell and Bretherton (1968) point out, the oscillation was produced by a systematic bias due to the omission of the linear terms in the balance equation. For the height variations shown in figure 2, these terms are included. Experiments with a geostrophic form and the linear form of the balance equation produced no change in the oscillation, although somewhat different initial fields resulted.

The apparent origin of the height oscillation on the boundaries of the region suggests that matching of boundary conditions in the diagnostic phase to those in the prognostic phase may not be sufficient. Particularly at the northern wall, the tendency was to reduce the geopotential in the high pressure region, thus reducing the height gradient along the wall. In experiment I, the first guess field for relaxation of the initial geopotential fields was obtained by differential analysis. Values on the boundary were computed with the hydrostatic equation using preliminary temperature analyses. In experiment II, the heights along the walls were set equal to constant values derived by averaging the initial-guess heights along the walls. This restriction further deteriorates the representativeness of the initialization, particularly in the upper levels. Examination of height deviation fields for experiment II showed that large height rises and falls on the walls were eliminated. The deviations which remained were nearly uniform along the walls and represent a slow "sloshing" from one wall to the other with a maximum value of about 8 m at 1000 mb.

Another detrimental aspect of the computationally produced oscillation is shown in figure 4. Because of the cyclic continuity in the zonal direction and eq (11), the area average of the vertical velocity is zero. The root-mean-square (rms) of the vertical velocity at the 1000-, 500-, and 200-mb levels rapidly oscillates in experiment I, especially at 1000 mb. The average rms value of 6×10^{-4} mb/s at 1000 mb is also significant, as most latent heat parameterization schemes depend on the vertical velocity at the top of the boundary layer. At higher levels, the average rms values are larger, but the dominant variations appear to have longer periods. In experiment II these longer period variations at upper levels remain, but with smaller median values. The rms vertical velocity at 1000 mb has approximately the same amplitude with a smaller high frequency component. It is clear that removal of the short-period height oscillation does not completely eliminate the large vertical velocity variations. This period of ω is related to the kinetic energy oscillation.

4. KINETIC ENERGY OSCILLATION

Early tests of the prediction model with barotropic analytical fields verified the conservation of kinetic energy properties of the finite-difference scheme. However, both adiabatic and diabatic experiments with real data produced a kinetic energy oscillation with a period of 19 hr. The amplitude of the kinetic energy oscillation was large relative to changes induced by baroclinic processes enhanced by diabatic heating and thus could not be ignored.

Figure 5 illustrates the kinetic energy oscillation at selected levels in experiments I and II. The kinetic energy variation with time in experiment II is smoother and has a slightly smaller amplitude. Most of the variation occurs at 250 mb, the level of maximum westerlies, and at 950 mb, the level of maximum easterlies. Intermediate layers have

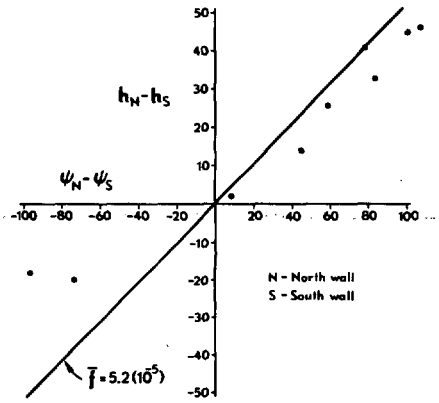

FIGURE 6.—Difference in stream function (10^{-5} $m^2 \cdot s^{-1}$) and heights (h) in meters between the north (N) and south (S) walls for experiment II. The solid line represents a geostrophic relation using the mean Coriolis acceleration for the channel.

small fluctuations, that suggest an oscillation in the kinetic energy of the zonal component.

The character of the wind oscillation suggested an imbalance between the north-south gradients of height and of the stream function (ψ) in the initial data. As shown in figure 6 for experiment II where the two gradients are constant for each level, most of the levels within the easterly basic flow fall along the line corresponding to a geostrophic initial basic current. At upper levels the gradients reverse, as the basic flow is westerly. An accumulation of errors in the first-guess height field, used to estimate the constant boundary heights, leads to an imbalance with the initial wind field, which is based on rather few reports at upper levels. Meridional pressure gradients at individual points are only slightly out of balance with the winds, at least below the tolerance of the relaxation scheme. However, the error is generally uniform across the channel. By using winds for initialization, the kinetic energy is fixed and the total height gradient is imposed. As these boundary heights are not fixed in time, an adjustment occurs which tends to balance wind and height gradients. As the boundary heights vary under the constraint that the mean height is conserved, the north-south height gradient will tend to change in the same sense at all points. Thus, there is a net change in the kinetic energy rather than a shift from zonal to meridional types of kinetic energy associated with the height oscillation.

Forcing the initial stream function and height boundary values to be balanced in a quasi-geostrophic sense eliminates the long-period kinetic energy oscillation (exp. III in fig. 5). Stream function gradients were specified that correspond to a smooth variation in the basic current, and the corresponding height gradients were chosen to assure smoothly varying temperature profiles. The temperature lapse rates at both the north and south walls are quite sensitive to small variations in the heights, or thicknesses between the layers. At the southern wall, the lapse rates were made to approximate the mean tropical sounding (Riehl 1954). A colder but smooth temperature profile results on the northern wall with the required height gradient. A rather marked decrease in the rms ω is noted in figure 4 for experiment III. The long-period oscillation at 200 mb is eliminated as well as much of the shorter period variations. An oscillation with a period of about 5 hr remains in the 500- and 200-mb rms ω values. This upper tropospheric oscillation is not too important, at least in the tests of the latent heat parameterization schemes. Økland (1970) found similar oscillations in the rms ω that seem to result from the absence of initial divergence.

5. DISCUSSION

Specifying inconsistent height boundary conditions in the diagnostic initialization of a 10-level primitive-equation model generated two separate types of oscillation that mask the meteorological developments. The height oscillation has a vertical structure similar to the inertial-gravity wave produced in a middle-latitude model, as discussed by Benwell and Bretherton(1968). However, the horizontal variation is such that the mean height remains constant within 0.25 m. Elimination of the height oscillation is achieved by setting boundary conditions that the initial heights along the northern and southern walls are constant. The oscillation in the total kinetic energy is not easily detected on the synoptic maps as the variation is in the basic current. This arises from an imbalance between the initial basic current and the specified height difference between the northern wall and the southern wall. When properly balanced height gradients between the walls are specified in the initialization, the kinetic energy oscillation is eliminated. Both the height oscillation and the kinetic energy oscillation have associated vertical velocity variations that are significant for models in which the parameterization of latent heating is dependent upon the vertical velocity. The rms ω is decreased by a factor of at least five when the suggested boundary conditions are incorporated.

The above discussion indicates the sensitivity of this particular primitive-equation model to the initial boundary conditions. In this case, the model is intended for prediction within a limited region of the Tropics, and the initialization is from winds. Considerable care must be taken in specifying the initial height fields on the boundaries to be consistent with the prediction model.

We have not considered the effects of specifying these required height boundary conditions on the representativeness of the initial data. It may be that the errors thus produced near the boundaries will rapidly deteriorate the accuracy of the predicted fields. The indication, with only a single set of initial data, is that this does not seem to be the case as the meteorological developments are rather slow. However, the implied inaccuracy of the initial fields, in addition to the errors from using only the nondivergent components of the wind, may be sufficient to reduce the verification statistics below other forecast schemes. This will likely be true in undisturbed regions of the Tropics, but near developing disturbances which

are capable of being simulated by the model, the predictive value may be substantial. Clearly, predictions with many sets of data will be required to determine the usefulness of primitive-equation models for limited regions of the Tropics.

ACKNOWLEDGMENTS

The authors thank their associates in the Department of Meteorology, Naval Postgraduate School, and especially Professor R. T. Williams, for assistance during the course of this research.

REFERENCES

Arakawa, Akio, "Computational Design for Long-Term Numerical Integration of the Equations of Fluid Motion: Two-Dimensional Incompressible Flow, Part I," *Journal of Computational Physics*, Vol. 1, No. 1, Jan. **1966**, pp. 119–143.

Benwell, G. R. R., and Bretherton, F. P., "A Pressure Oscillation in a Ten-Level Atmospheric Model," *Quarterly Journal of the Royal Meteorological Society*, Vol. 94, No. 400, London, England, Apr. **1968**, pp. 123–131.

Brown, John A., Jr., "Numerical Experimentation in Data Initialization for the Primitive Equations (Abstract)," *Bulletin of the American Meteorological Society*, Vol. 51, No. 1, Jan. **1970**, p. 80.

Charney, Jule, and Eliassen, Arnt, "On the Growth of the Hurricane Depression," *Journal of the Atmospheric Sciences*, Vol. 21, No. 1, Jan. **1964**, pp. 68–75.

Hawkins, Harry F., and Rosenthal, Stanley L., "On the Computation of Stream Functions From the Wind Field," *Monthly Weather Review*, Vol. 93, No. 4, Apr. **1965**, pp. 245–252.

Krishnamurti, T. N., "An Experiment in Numerical Prediction in Equatorial Latitudes," *Quarterly Journal of the Royal Meteorological Society*, Vol. 95, No. 405, London, England, July **1969**, pp. 594–620.

Kuo, H.-L., "On Formation and Intensification of Tropical Cyclones Through Latent Heat Release by Cumulus Convection," *Journal of the Atmospheric Sciences*, Vol. 22, No. 1, Jan. **1965**, pp. 40–63.

Landis, Robert C., and Leipper, Dale F., "Effects of Hurricane Betsy upon Atlantic Ocean Temperature, Based upon Radio-Transmitted Data," *Journal of Applied Meteorology*, Vol. 7, No. 4, August **1968**, pp. 554–562.

Murakami, Takio, "Initial Adjustment of Data in the Tropics," *Report* HIG–69–23, Hawaii Institute of Geophysics, Honolulu, Nov. **1969**, 54 pp.

Økland, Hans, "On the Adjustment Toward Balance in Primitive Equation Weather Prediction Models," *Monthly Weather Review*, Vol. 98, No. 4, Apr. **1970**, pp. 271–279.

Pearce, R. P., and Riehl, H., "Parameterization of Convective Heat and Momentum Transfer Suggested by Analysis of Caribbean Data," *Proceedings of the WMO/IUGG Symposium on Numerical Weather Prediction, Tokyo, Japan, November 26–December 4, 1968*, Japan Meteorological Agency, Tokyo, Mar. **1969**, pp. I–75—I–84.

Riehl, Herbert, *Tropical Meteorology*, McGraw-Hill Book Co., Inc., New York, N.Y., **1954**, 392 pp.

Rosenthal, Stanley L., "Numerical Experiments With a Multilevel Primitive Equation Model Designed to Simulate the Development of Tropical Cyclones: Experiment I," *ESSA Techincal Memorandum* ERLTM–NHRL 82, U.S. Department of Commerce, National Hurricane Research Laboratory, Miami, Fla., Jan. **1969**, 36 pp.

[*Received December 11, 1970; revised May 13, 1971*]